

# ImagineMap: Enhanced HD Map Construction with SD Maps

Yishen Ji

Zhiqi Li  
Nanjing University

Tong Lu

December 22, 2024

## Abstract

Track Mapless demands models to process multi-view images and Standard-Definition (SD) maps, outputting lane and traffic element perceptions along with their topological relationships. We propose a novel architecture that integrates SD map priors to improve lane line and area detection performance. Inspired by TopoMLP, our model employs a two-stage structure: perception and reasoning. The downstream topology head uses the output from the upstream detection head, meaning accuracy improvements in detection significantly boost downstream performance.

## 1. Introduction

Driving without High-Definition (HD) maps requires a vehicle to possess a high level of active scene understanding capability. This challenge aims to explore the limits of scene reasoning. Neural networks need to process multi-view images and Standard-Definition (SD) maps, and output perception results of lanes and traffic elements, while simultaneously providing topological relationships among lanes and between lanes and traffic elements. This means that the neural network must not only identify lanes and various traffic elements on the road but also understand the interrelationships and positional relationships between them, thereby enhancing the driving capability of autonomous systems in the absence of HD map support.

In this work, we propose a novel architecture that integrates SD map priors into the model, thereby enhancing the performance of lane line and area detection. Our overall model design is inspired by TopoMLP [11] and employs a two-stage structure, perception and reasoning. The downstream topology head takes the output of the upstream detection head as its input, meaning that improvements in the accuracy of the detection head will significantly boost the performance of the downstream head. We utilize DETR for constructing the lane segment detection head and deformable DETR for constructing the traffic element head.

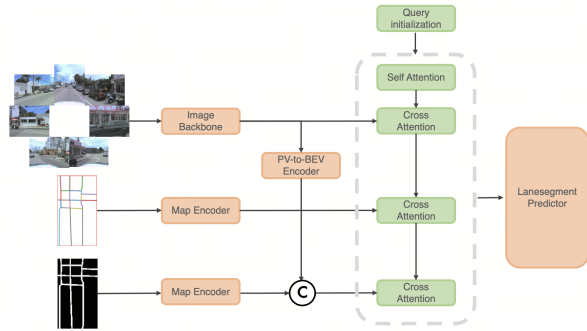


Figure 1. The structure for incorporating SD map information into detection. Map encoder extracts SD map features to interact with lane queries via cross-attention. Additionally, we rasterize SD map to generate a mask, whose features are extracted by a small map backbone and concatenated with BEV features from BEV encoder for further interaction with lane queries.

## 2. Method

### 2.1. LaneSegment Detection

Our lane detection head is based on LaneSegNet[4] and adopts the DETR[2] structure. Each lane segment includes three lines, a centerline and its corresponding left and right boundaries, and each line is represented by a series of evenly spaced three-dimensional points. The number of sample points for each line is  $N_p$ . We adopt instance query to represent the lane segment.

By utilizing the position and posture information of ego vehicle, we obtain the SD map (vectorized) within the BEV range. To fully harness the information provided by the SD map, we incorporate it into our detection process in two ways. First, we employ SMERF[9], a powerful transformer-based encoder, to extract the SD map features. These are then used as queries to interact with the lane queries through cross-attention. Next, we grid the SD map to generate a mask and extract its features through a small network(ResNet-18). These features are concatenated with

the BEV features constructed by BEVFormer[5] and again interact with the lane queries through cross-attention. The specific structure is illustrated in Figure 1.

To further leverage semantic and geometric information, we introduce auxiliary foreground segmentation on bird’s eye view (BEV). The entire lane segment area (bounded by the left and right lane lines) is considered as the segment mask range.

We use Focal loss for the class head and L1 loss for the lane head. We introduced a lane line type classification loss using Cross Entropy Loss. BEV seg loss is composed of mask loss(Cross Entropy Loss) and dice loss. Thus, the overall lanesegment loss function can be formulated as:

$$L_{ls} = \lambda_{cls}L_{cls} + \lambda_{reg}L_{reg} + \lambda_{type}L_{type} + \lambda_{mask}L_{mask} + \lambda_{dice}L_{dice} \quad (1)$$

where  $\lambda_{cls}, \lambda_{reg}, \lambda_{type}, \lambda_{mask}, \lambda_{dice}$  is set to 1.5, 0.0025, 0.1, 3.0 and 3.0 respectively.

## 2.2. Area Detection

We implemented the area detection task based on MapTr[6] structure.

Similar to the way we utilize the sd map prior in lane detection task, we pass the sd map through a separate map encoder, and then perform cross-attention with the query on the features.

Auxiliary BEV segmentation supervision is also adopted in this task. But unlike in the lane detection task where the entire lane segment is considered for segmentation, the area mask is only taken along the instance boundary.

The area detection head is supervised by  $L_a$ , which is composed of a classification loss  $L_{cls}$  (Focal Loss), a regression loss  $L_{reg}$  (L1 Loss), a direction loss  $L_{dir}$  (Points Direction Cosine Loss) and auxiliary seg loss  $L_{seg}$  (Cross Entropy Loss):

$$L_a = \lambda_{cls}L_{cls} + \lambda_{reg}L_{reg} + \lambda_{dir}L_{dir} + \lambda_{seg}L_{seg} \quad (2)$$

where  $\lambda_{cls}, \lambda_{reg}, \lambda_{dir}, \lambda_{seg}$  is set to 1.5, 0.0025, 0.005, 10 respectively.

## 2.3. Traffic Element Detection

Our traffic element detection head follows the head design in Deformable DETR[12] to predict bounding boxes and classification scores. The detection head takes the front-view image features as input. To improve the accuracy of the detection head, we use Co-DETR[13], a powerful object detection model, to generate proposals. Co-DETR is a novel collaborative hybrid assignments training scheme for more efficient and effective DETR-based detectors. This

scheme enhances the learning ability of the encoder in end-to-end detectors through training multiple parallel auxiliary heads supervised by one-to-many label assignments. It also improves the attention learning of the decoder by conducting extra customized positive queries, extracting the positive coordinates from these auxiliary heads.

The traffic elements detection head is supervised by  $L_{te}$ , which decomposed into a classification loss  $L_{cls}$  (Focal Loss), a regression loss  $L_{reg}$ , and an IoU loss  $L_{iou}$  (GIoU):

$$L_{te} = \lambda_{cls}L_{cls} + \lambda_{reg}L_{reg} + \lambda_{iou}L_{iou} \quad (3)$$

where  $\lambda_{cls}, \lambda_{reg}, \lambda_{iou}$  is set to 1.0, 2.5, 1.0 respectively.

## 2.4. Topology Lane-lane

The lane-lane topology reasoning branch aims to predict the connection relationship between lanes. To incorporate the distinct lane information, we integrate the predicted lane points into the lane query features. We use a MLP to embed the lane coordinates and then add them to the decoded lane query features. The lane-lane topology head is supervised by  $L_{ll}$  (Focal Loss), with a weight of 5.

## 2.5. Topology Lane-Traffic

Lane-traffic topology head is also an MLP structure but simultaneously takes inputs from both the lane head and the traffic head. The lane-traffic topology head is supervised by  $L_{lt}$  (Focal Loss), with a weight of 5.

## 3. Experiments

### 3.1. Dataset and Metrics

OpenLane-V2 is the first dataset on topology reasoning for traffic scene structure. This dataset utilizes multi-view images as input and encompasses a range of tasks, which include the perception of lane lines and traffic elements, the detection of specific areas, and the prediction of topological relationships between lane lines as well as between lane lines and traffic elements. OpenLane-V2 is constructed on the base of two existing datasets: Argoverse 2[10] (subset A) and nuScenes[1] (subset B). In scenarios involving map-less tracks, we employ the subset A dataset.

For subset A, the resolution of input images is 2048 × 1550, except for the front-view image, whose resolution is 1550 × 2048. The number of scene segment for Train set, Val set and Test set is 700, 150 and 150. And the annotation range for the dataset is +50 meters in x-axis and +25 meters in y-axis(for the vehicle coordinate system)

The evaluation system utilizes OpenLane-V2 UniScore (OLUS) as the final metric, which is the average of various metrics covering different aspects of the primary task. The calculation for OLUS is as follows:

$$OLUS = \frac{1}{5}[DET_l + DET_a + DET_t + \sqrt{TOP_{ll}} + \sqrt{TOP_{lt}}]$$

$DET_l$ : lanesegment prediction with Frechet(for centerline) and Chamfer(for left and right laneline) based mAP;  $DET_a$ : area prediction with Chamfer based mAP;  $DET_t$ : traffic element prediction IOU based mAP;  $TOP_{ll}$ : mAP on topology among lane segments;  $TOP_{lt}$ : mAP on topology between lane segments and traffic elements;

It is important to note that this year’s metrics differ from that of last year. The task of lane detection now includes the centerline and the left and right lanelines. Moreover, there’s a new prediction task: area, namely pedestrian crossings and road boundaries, are regarded as undirected curves, which are closed or intersected with the boundaries of the BEV range.

### 3.2. Experimental Details

Initially, the front-view image is cropped to a size of  $1550 \times 1550$ . Subsequently, all images are scaled down by a factor of 0.75 as the input to backbone to achieve a balance between performance and training speed.

We utilize the powerful EVA02 [3] as our backbone to extract multi-view image features, which are then used in the lane segment (ls) head and traffic element (te) head (te head only uses features from the front-view image). We build the bird’s eye view (BEV) features using BEVFormer[5], and the number of encoder layer is set as 6. Increasing the size of BEV features can also improve the performance of lane detection and area detection. We increased it from  $200 \times 100$  to  $400 \times 200$ . However, this will correspondingly require more computational resources.

We adopt the AdamW optimizer and a cosine annealing schedule with an initial learning rate of  $4e-4$ . Our proposed method is trained for 24 epochs with a batch size of 1, using 16 NVIDIA Tesla A100 GPUs. We also employ layer decay to prevent overfitting and accelerate convergence.

### 3.3. Lane Detection

We found that the detection performance is optimal when the number of sampling points  $N_p$  for each lane query matches the number of points in the annotations. We set  $N_p = 11$ . And number of instance query is 300.

We tested the impact of different auxiliary methods on lane detection performance on the test set, as shown in Table 1.

### 3.4. Area Detection

Abalation on area detection is shown in Table 2.

Fine tune can further improve the performance of area head. We freeze the other parts of the model and train the area head for another 24 epochs using a smaller learning rate.

Method	mAP (%)
Base	32.22
+ EVA02 + Layer Decay	35.03
+ BEV Scale Up	37.66
+ Scale 0.75	39.08
+ Aux BEV Seg Sup	42.95

Table 1. Ablation of lanesegment detection on OpenLane-V2 test set.

Method	mAP (%)
Base	20.52
+ EVA02 Layer Decay	23.46
+ BEV Scale Up	26.59
+ SD Map Query	28.00
+ Scale 0.75	30.76
+ Aux BEV Seg Sup	32.00
+ Fine Tune	34.72

Table 2. Ablation of area detection on OpenLane-V2 test set.

### 3.5. Traffic Element Detection

Introducing proposals generated by Co-DETR significantly improved the traffic element detection performance. To apply Co-DETR on OpenLane-V2 dataset, we first get all of the front-view images from multi-view images (and corresponding ground truth), then reformat them according to the COCO[7] dataset format. Input images is cropped into  $1550 \times 1550$  for training efficiency. We tested the performance of two strong backbones. Using Swin-L [8] to generate proposals, TE detection performance achieved 79.15. In contrast, using ViT-L to generate proposals, TE detection performance improved to 82.15, which is shown in Table 3.

Method	mAP (%)
Base	67.47
+ proposal	79.15
+ vit-L	82.15

Table 3. Ablation of traffic element detection on OpenLane-V2 test set.

### 3.6. Topology

As shown in Table 4 and Table 5, methods that improve the performance of upstream detection heads can effectively enhance the reasoning performance of the topology heads.

Method	mAP (%)
Base	29.99
+ EVA02 Layer Decay	31.57
+ lane query300	36.48

Table 4. Ablation of lane-lane topology on OpenLane-V2 test set.

Method	mAP (%)
Base	32.98
+ TE proposal	37.56
+ EVA02 Layer Decay	40.64
+ lane query300	41.91

Table 5. Ablation of lane-traffic topology on OpenLane-V2 test set.

## References

- [1] Holger Caesar, Varun Bankiti, Alex H Lang, Sourabh Vora, Venice Erin Liong, Qiang Xu, Anush Krishnan, Yu Pan, Giancarlo Baldan, and Oscar Beijbom. nuscnets: A multi-modal dataset for autonomous driving. In *Proceedings of the IEEE/CVF conference on computer vision and pattern recognition*, pages 11621–11631, 2020. 2
- [2] Nicolas Carion, Francisco Massa, Gabriel Synnaeve, Nicolas Usunier, Alexander Kirillov, and Sergey Zagoruyko. End-to-end object detection with transformers. In *European conference on computer vision*, pages 213–229. Springer, 2020. 1
- [3] Yuxin Fang, Quan Sun, Xinggang Wang, Tiejun Huang, Xinlong Wang, and Yue Cao. Eva-02: A visual representation for neon genesis. *arXiv preprint arXiv:2303.11331*, 2023. 3
- [4] Tianyu Li, Peijin Jia, Bangjun Wang, Li Chen, Kun Jiang, Junchi Yan, and Hongyang Li. Laneseqnet: Map learning with lane segment perception for autonomous driving. *arXiv preprint arXiv:2312.16108*, 2023. 1
- [5] Zhiqi Li, Wenhai Wang, Hongyang Li, Enze Xie, Chonghao Sima, Tong Lu, Yu Qiao, and Jifeng Dai. Bevformer: Learning bird’s-eye-view representation from multi-camera images via spatiotemporal transformers. In *European conference on computer vision*, pages 1–18. Springer, 2022. 2, 3
- [6] Bencheng Liao, Shaoyu Chen, Xinggang Wang, Tianheng Cheng, Qian Zhang, Wenyu Liu, and Chang Huang. Maptr: Structured modeling and learning for online vectorized hd map construction. *arXiv preprint arXiv:2208.14437*, 2022. 2
- [7] Tsung-Yi Lin, Michael Maire, Serge Belongie, James Hays, Pietro Perona, Deva Ramanan, Piotr Dollár, and C Lawrence Zitnick. Microsoft coco: Common objects in context. In *Computer Vision—ECCV 2014: 13th European Conference, Zurich, Switzerland, September 6–12, 2014, Proceedings, Part V 13*, pages 740–755. Springer, 2014. 3
- [8] Ze Liu, Yutong Lin, Yue Cao, Han Hu, Yixuan Wei, Zheng Zhang, Stephen Lin, and Baining Guo. Swin transformer: Hierarchical vision transformer using shifted windows. In *Proceedings of the IEEE/CVF international conference on computer vision*, pages 10012–10022, 2021. 3
- [9] Katie Z Luo, Xinshuo Weng, Yan Wang, Shuang Wu, Jie Li, Kilian Q Weinberger, Yue Wang, and Marco Pavone. Augmenting lane perception and topology understanding with standard definition navigation maps. *arXiv preprint arXiv:2311.04079*, 2023. 1
- [10] Benjamin Wilson, William Qi, Tanmay Agarwal, John Lambert, Jagjeet Singh, Siddhesh Khandelwal, Bowen Pan, Ratnesh Kumar, Andrew Hartnett, Jhony Kaesemodel Pontes, et al. Argoverse 2: Next generation datasets for self-driving perception and forecasting. *arXiv preprint arXiv:2301.00493*, 2023. 2
- [11] Dongming Wu, Jiahao Chang, Fan Jia, Yingfei Liu, Tiancai Wang, and Jianbing Shen. Topomlp: An simple yet strong pipeline for driving topology reasoning. *arXiv preprint arXiv:2310.06753*, 2023. 1
- [12] Xizhou Zhu, Weijie Su, Lewei Lu, Bin Li, Xiaogang Wang, and Jifeng Dai. Deformable detr: Deformable transformers for end-to-end object detection. *arXiv preprint arXiv:2010.04159*, 2020. 2
- [13] Zhuofan Zong, Guanglu Song, and Yu Liu. Detsr with collaborative hybrid assignments training. In *Proceedings of the IEEE/CVF international conference on computer vision*, pages 6748–6758, 2023. 2